Vibro-acoustic FEA for an Effect of a Sail in Automotive Seat Structures Including Poroelastic Materials and Metal Frames

Takao Yamaguchi[1, a], Toru Fukushima[1,b], Takashi Yamamoto[2,c], Masashi Fujimoto[1,d] and Ikuo Shirota[1,e]

[1]Gunma University, 1-5-1 Tenjin-cho, Kiryu, Gunma, 376-8515 Japan

[2]Kogakuin University, 2665-1 Nakano, Hachioji, Tokyo 192-0015 Japan

[a]<yamagme3@gunma-u.ac.jp>, [b]<t14806006@gunma-u.ac.jp>, [c]<takashi_yamamoto@cc.kogakuin.ac.jp>, [d]<t07801239@gunma-u.ac.jp>, [e]<t06801422@gunma-u.ac.jp>

Keywords: finite element method, poroelastic material, numerical simulation, vibro-acoustic problem.

Abstract. This report deals with vibro-acoustic analysis using three-dimensional FEM for automotive seat structures having poroelastic materials and metal frames. There are two media (i.e. internal air and a resin block) in the poroelastic materials for the seat. By carrying out numerical analysis related to the model test, the poroelastic materials for the automotive seat had sound absorption effects for cavity resonance in a room. Further the poroelastic materials also had damping effects for the structural resonance of the metal seat frame under impact excitation at the metal frame. Furthermore, under an acoustic excitation, vibration amplitudes of the metal frame increase by attaching the poroelastic materials to the metal frame. It is " an effect of a sail'' of the resin block in the poroelastic material, which increases vibration level of the seat metal frame by receiving sound pressure. This effect can be simulated using Biot model for the poroelastic materials.

1. Introduction

It is known that interior parts of cabins in automobiles have significant influences on the interior noise [1]. The interior parts are constituted of elastic materials, viscoelastic materials and porous materials. Therefore, vibration and acoustic analysis in consideration of the mixed materials are required. A seat structure has the largest surface area among interior parts in the cabin. Thus, it is necessary to clarify the dynamic characteristics of the seat structure in order to improve accuracy of the predicted interior noise level.

In relatively low frequency range where modal density is low, numerical analysis is effective since numerical methods under diffused sound field, cannot be applicable to the interior noise in the low or middle frequency regions because wavelengths are not smaller than the size of the automotive structures and sound fields.

The seat structure for automobiles is mainly composed of metal frames, porous materials (e.g. urethane foams) and surface materials. In actual cars, the seat has a complicated structure for vibration and acoustic analysis because there exist many movable parts (e.g. parts of sliding mechanism and links).

The porous material for the seat has two media for wave propagation. One is a viscoelastic resin block of the seat foam. The other is an internal air of the foam. For the numerical model of the foam, we mainly used Biot type poroelastic model for the seat because there are the two media. We use a simplified model for the automotive seat structures and perform three-dimensional finite element analysis to investigate vibro-acoustic coupling in the seat structure under the condition without the

surface materials on the foam. Further, experiments are also carried out to verify the numerical results. Note that the simplified model includes no sliding mechanism and no links.

2. Numerical procedure

2.1 Discrete Equations of Vibration for the Internal Air and the Viscoelastic Resin Block of the Seat Foam

We use Biot model for the foam of the seat as a poroelastic material. By using this model, the coupling between sound pressure of the internal air and viscoelastic deformation of the resin block of the foam can be considered [2, 3, 4, 5, 6].

Firstly, the equations of motion for the internal air of the foam are as follows:

$$-\omega^2(\rho_{21}u_x+\rho_{22}U_x)+j\omega b(U_x-u_x)=-\Omega(\partial p/\partial x) \tag{1}$$

$$-\omega^2(\rho_{21}u_y+\rho_{22}U_y)+j\omega b(U_y-u_y)=-\Omega(\partial p/\partial y) \tag{2}$$

$$-\omega^2(\rho_{21}u_z+\rho_{22}U_z)+j\omega b(U_z-u_z)=-\Omega(\partial p/\partial z) \tag{3}$$

Where, $\{u\}=\{u_x,u_y,u_z\}^T$ and $\{U\}=\{U_x,U_y,U_z\}^T$ are the displacement of the viscoelastic resin block and the particle displacement of the internal air, respectively. $\rho_{21}=-\rho_a$, $\rho_a=\rho_f(s-1)$, s is the tortuosity, $\rho_f=\rho_0\Omega$, ρ_0 is the mass density of the air, Ω is the porosity, $\rho_{22}=\rho_f+\rho_a$, $b=\Omega r$ and r is the flow resistance.

Secondly, the equations of motion for the viscoelastic resin block of the foam are as follows:

$$-\omega^2(\rho_{11}u_x+\rho_{12}U_x)+j\omega b(u_x-U_x)=(\partial\sigma_x/\partial x)+(\partial\tau_{xy}/\partial y)+(\partial\tau_{xz}/\partial z) \tag{4}$$

$$-\omega^2(\rho_{11}u_y+\rho_{12}U_y)+j\omega b(u_y-U_y)=(\partial\sigma_y/\partial y)+(\partial\tau_{yz}/\partial z)+(\partial\tau_{yx}/\partial x) \tag{5}$$

$$-\omega^2(\rho_{11}u_z+\rho_{12}U_z)+j\omega b(u_z-U_z)=(\partial\sigma_z/\partial z)+(\partial\tau_{zx}/\partial x)+(\partial\tau_{zy}/\partial y) \tag{6}$$

Where, $\rho_{11}=\rho_s+\rho_a$ $\rho_{12}=-\rho_a$, $\rho_s=\rho_1(1-\Omega)$ and ρ_1 is the mass density of the resin skeleton. σ_x and σ_y are the normal stresses in *x* and *y* directions, respectively. τ_{xy} is the shear stress.

Continuity equation of the internal air of the foam is as follows.

$$-\Omega p=Q_m\ div\{u\}+E_m\ div\{U\} \tag{7}$$

Where, $E_m=\Omega E^*$, E^* is the bulk modulus of elasticity for the internal air. $Q_m=(1-\Omega)E^*$ is the coupling modulus of elasticity.

The relation between stress and strain for the viscoelastic resin block of the foam is as follows.

$$\sigma_x=2G_s^*(\partial u_x/\partial x)+A_s^*div\{u\}+Q_m\ div\{U\} \tag{8}$$

$$\sigma_y=2G_s^*(\partial u_y/\partial y)+A_s^*div\{u\}+Q_m\ div\{U\} \tag{9}$$

$$\sigma_z=2G_s^*(\partial u_z/\partial z)+A_s^*div\{u\}+Q_m\ div\{U\} \tag{10}$$

$$\tau_{xy}=\tau_{yx}=G_s^*((\partial u_x/\partial y)+(\partial u_y/\partial x)) \tag{11}$$

$$\tau_{yz}=\tau_{zy}=G_s^*((\partial u_y/\partial z)+(\partial u_z/\partial y)) \tag{12}$$

$$\tau_{zx}=\tau_{xz}=G_s^*((\partial u_z/\partial x)+(\partial u_x/\partial z)) \tag{13}$$

Where, $G_s^* = E_s(1+j\eta_s)/2(1+\nu_s)$, $A_s^* = E_s\nu_s(1+j\eta_s)/((1+\nu_s)(1+2\nu_s))$. G_s^* is the shear modulus of elasticity of the resin block. E_s, η_s and ν_s are the storage modulus of elasticity, the material loss factor and Poisson's ratio, respectively.

Deleting sound pressure *p* from Eqs. (1), (2) and (3), we obtain simultaneous differential equations with respect to $\{U\}$ and $\{u\}$.

Next, using a shape function $[N_U]^T$ for the internal air of the foam, the relation between the particle displacement $\{U\}$ in an element and the nodal particle displacement $\{U_e\}$ is approximated as follows.

$$\{U\} = [N_U]^T \{U_e\} \tag{14}$$

Similarly, using a shape function $[N_u]^T$ for the viscoelastic resin block of the foam, the relation between the displacement $\{U\}$ of the resin block in an element and the nodal displacement $\{U_e\}$ is approximated as follows.

$$\{u\} = [N_u]^T \{u_e\} \tag{15}$$

The equations (14) and (15) are substituted into the simultaneous differential equations with respect to $\{U\}$ and $\{u\}$. Then, applying Galerkin's procedure to the obtained equations, the following discrete equations can be obtained.

$$-\omega^2([M_{11}]\{u_e\}+[M_{12}]\{U_e\}) + j\omega([C_{11}]\{u_e\}+[C_{12}]\{U_e\}) + [K_{11}]\{u_e\}+[K_{12}]\{U_e\} = \{F_e\} \tag{16}$$

$$-\omega^2([M_{21}]\{u_e\}+[M_{22}]\{U_e\}) + j\omega([C_{22}]\{U_e\}+[C_{21}]\{u_e\}) + [K_{22}]\{U_e\}+[K_{21}]\{u_e\} = \{f_e\} \tag{17}$$

Where, $[M_{11}],[M_{12}],[M_{21}],[M_{22}]$ are the mass matrix and $[K_{11}],[K_{12}],[K_{21}],[K_{22}]$ are the stiffness matrix and $[C_{11}],[C_{12}],[C_{21}],[C_{22}]$ are the damping matrix of the Biot element.

2.2 Discrete Equations for the Metal Frame and the Closed Space

For the vibration of the metal frame, we used linear three-dimensional finite element model [7] having the complex stiffness matrix to consider hysteresis damping. For the sound field in a closed space of a cabin model, we used particle displacements as unknowns for the three-dimensional finite element [8, 9, 10].

2.3 Discrete Equations in the Global System

All elements for the system are superposed appropriately. This yields the discrete simultaneous equations to be solved in the global system.

3. Models for numerical analysis and test

Figure 1 shows an outline of the numerical model and the experimental device. We installed an aluminum frame and a urethane foam for the automotive seat structure into a small closed space. Figures 1(a) and (b) show finite element models without / with the foam, respectively. Figure 1(c) is a photo of the experimental device.

Figure 2 shows the detail geometry of the seat model composed of (a) the metal frame, (b) the foam and (c) the closed space. As shown in Fig. 2(a), the shape of the aluminum frame is like a ladder. The height and the width of the frame are 280[mm] and 120[mm], respectively. The shape of the cross section of the beams in the frame is square (10[mm]×10[mm]). We attached the foam to the aluminum frame using adhesive tapes. As illustrated in Fig. 2 (b), the height and the width of the

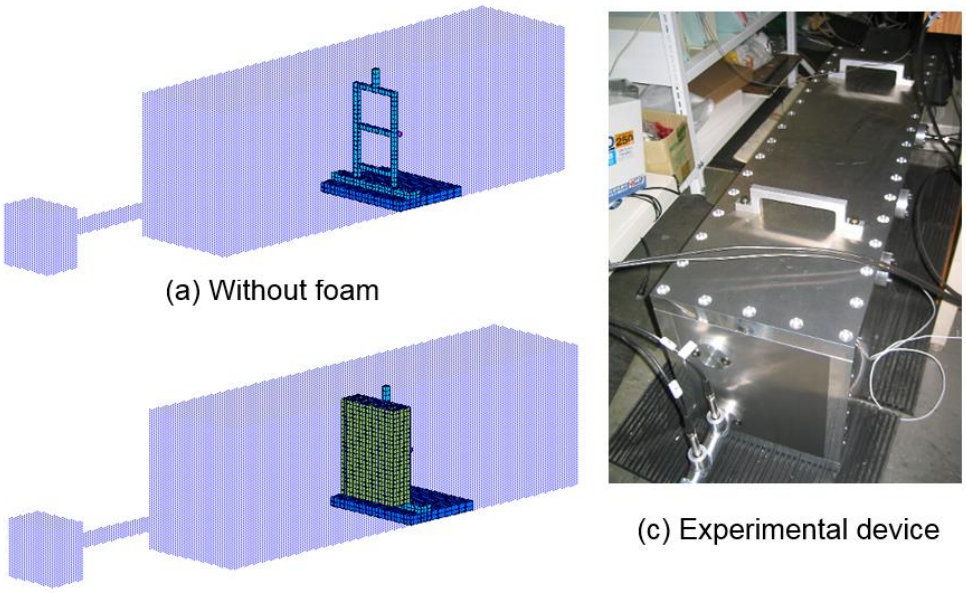

Fig.1 Outline of FEM model and experimental device

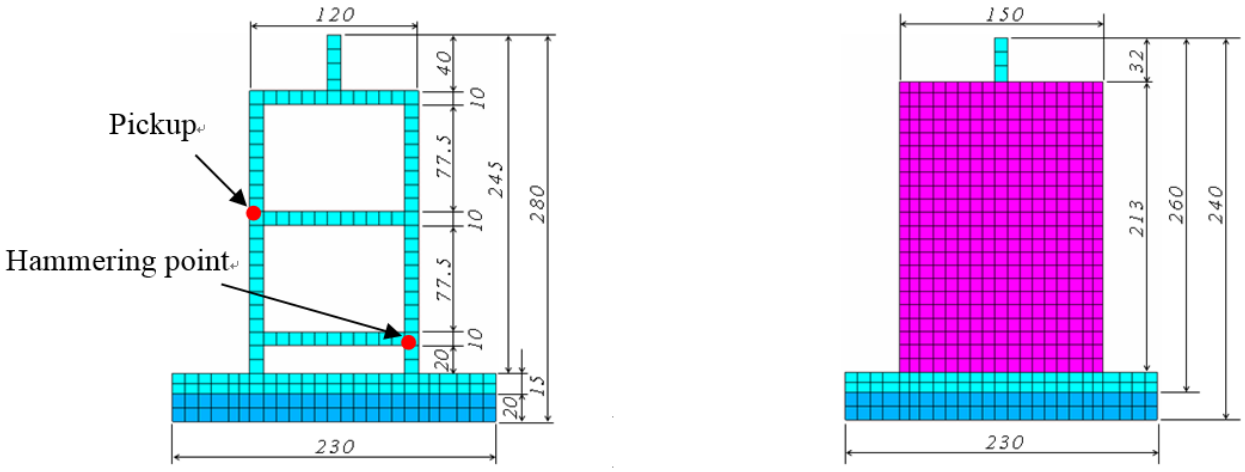

(a) Rear view of model without foam

(b) Front view of model with foam

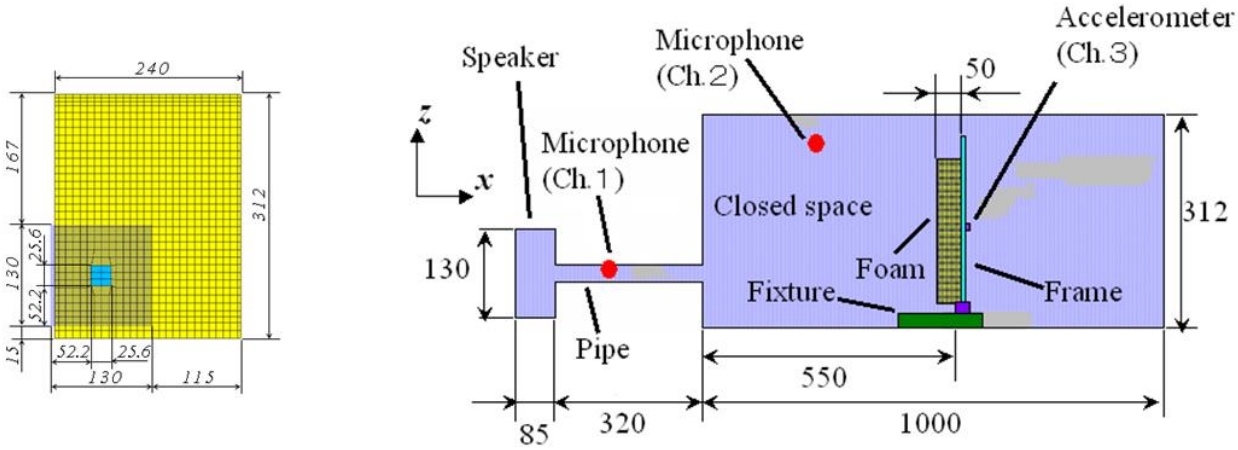

(c) Front and side views of seat model

Fig.2 Detail geometry of seat model

foam are 213[mm] and 150[mm], respectively. Thickness of the foam is 50[mm]. This foam is a typical material used in a seat structure in automobiles. The seat foam for this study is cut off from a larger block of the urethane foam. Thus, there exists no membrane on the surface of the seat foam. For the finite element model, we connect between the metal frame and the foam using complex spring elements to take the effects of the adhesive tape into consideration. Acoustic excitation is applied on this test model in the small closed space for the numerical analysis and experiment as shown in Fig. 2(c). The height and the width of the closed space are 312[mm]×240[mm]. The length of the closed space is 1000[mm]. Both sound pressure level of the space and acceleration level of the metal frame are observed and computed. The frequency range on this investigation is from 50[Hz] to 500[Hz]. This frequency range is corresponding to the range of road noise in cars where the coupling between the vibration of the automotive structures and the sound is strong. Note that the closed space cannot be regarded as diffused sound field, and the metal frame is also not regarded as diffused field because of their low modal density

4. Vibro-acoustic analysis of automotive seat structure

4.1 Vibration Analysis Using Hammer Excitation

By a hammering test, we observe transfer functions A/F between accelerations A of the frame and an input force F of the other point on the frame. Figure 2(a) shows the input point and the observation point. We compute the responses A/F using the finite element method under the same condition as the hammering test. Figure 3(a) is the experimental responses of the hammering test, and Fig. 3(b) is the corresponding calculated results. In the graphs of Fig. 3, there exist gains of A/F for the metal frame with / without the foam, respectively. According to Fig. 3(a), the first and the third peaks correspond to the first and the second bending modes in x-direction, respectively. The second peak is the first torsion mode around z-axis. The modal loss factor increases from 0.014[-] without the foam to 0.042[-] with the foam for the first peak. In the same manner, the foam improves the modal loss factor for the second peak from 0.0026[-] to 0.17[-]. The factor for the third peak increases from 0.030[-] to 0.086[-]. Thus, all peaks decrease due to vibration damping effect of the foam. The calculated results in Fig. 3(b) and the experimental ones in Fig. 3(a) agree well qualitatively.

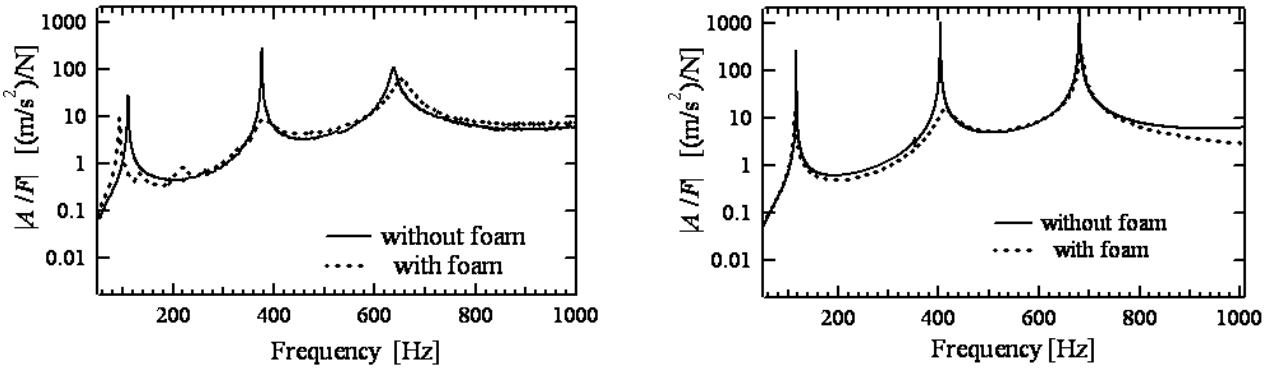

(a) Experiment (b) FEM

Fig. 3 Acceleration of frame under hammer excitation

4.2 Vibro-acoustic Analysis under Acoustic Excitation

As shown in Figs. 1 and 2, the metal frame with the foam is set in the closed space, and is excited by a speaker in the small box. This speaker box is connected to the closed space using a short pipe. Microphones are set at the connected pipe (i.e. Channel 1 as a reference point) and in the closed

space (i.e. Channel 2 as an observation point) as illustrated in the Fig. 2(c). We observe transfer functions P_2/P_1 between sound pressure of the Channel 1 and sound pressure of the Channel 2. Figure 4(a) shows the experimental result. In this figure, solid line shows sound pressure $|P_2/P_1|$ without the foam, while the dotted line shows the result with the foam. The first and second peaks of $|P_2/P_1|$ are the first and second cavity resonance in x-direction, respectively. The foam increases modal loss factor of the first peak from 0.0072[-] to 0.031[-]. Therefore, all peaks are damped due to sound absorption effect of the foam. As can be seen in the Fig. 4(b), the computed sound pressure $|P_2/P_1|$ corresponds to the experimental one quantitatively.

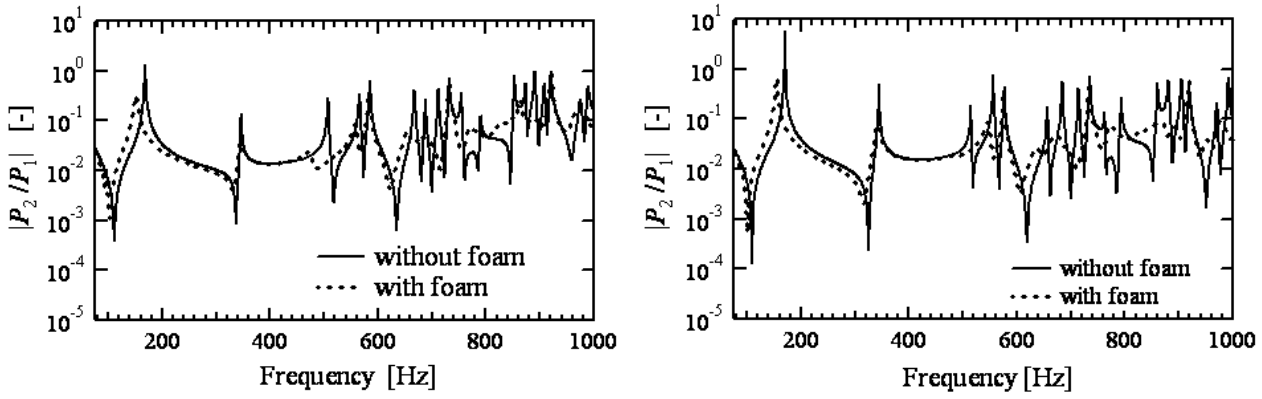

(a) Experiment (b) FEM

Fig. 4 Sound pressure in the closed space under acoustic excitation

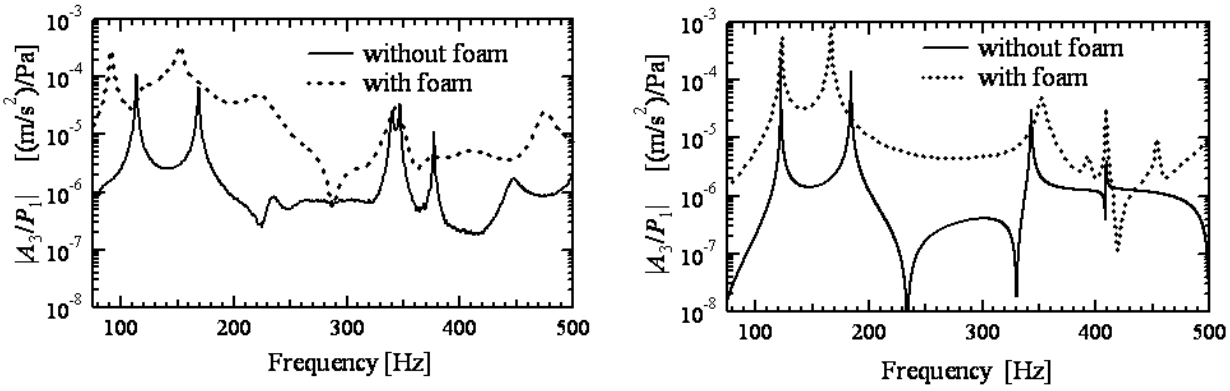

(a) Experiment (b) FEM

Fig. 5 An effect of a sail in acceleration of seat frame under acoustic excitation

Further, an accelerometer (i.e. Channel 3) is attached to the same position as the hammering test on the metal frame. Thus, we evaluate transfer function A_3 / P_1. Figure 5 (a) shows the experimental accelerations $|A_3 / P_1|$ with and without the foam. In this figure, the first peak corresponds to the first bending mode of the frame. This mode is the same mode as the first mode for the hammering test. With the foam, the modal loss factor of this mode increases from 0.0071[-] to 0.025[-] due to the damping effect of the foam. Thus, there exists the damping effect of the foam under the acoustic excitation. However, the amplitude of the acceleration increases, when the foam is attached to the metal frame. Namely, though damping increases due to the foam, the acceleration increases. The second peak in Fig. 5(a) is the first acoustic cavity mode in x-direction. This mode corresponds to the first mode in Fig. 4 (a). With the foam, the modal loss factor of this mode increases from 0.0068[-] to 0.034[-]. This implies that damping for this cavity mode improves due to the sound absorption effect

of the foam. Nevertheless, the amplitude of the acceleration $|A_3 / P_1|$ is amplified due to the foam. For this mode, though the damping increases due to the foam, the amplitude increases.

We think that it is " an effect of a sail'' of the foam, which increases vibration level of the seat metal frame by receiving sound pressure. Figure 5(b) shows computed results of the acceleration $|A_3 / P_1|$ using the Biot model for the seat foam. As can be seen, the amplitude of the metal frame is also amplified because of adhesion of the foam to the frame. This result is consistent with the experimental one. Figure 6 shows the calculated acceleration using the model of internal air for the foam without the effect of the viscoelastic resin block [8. 9, 10]. As shown in this figure, the amplitude of the frame's acceleration decreases due to the foam. This result is not consistent with the previous experimental one in Fig. 5(a). This implies that the viscoelastic resin block is significant influences on 'the effect of an sail'. To simulate this effect, it is necessary to use the Biot model, which considers the coupling between sound waves in the internal air and the vibration of the viscoelastic resin block.

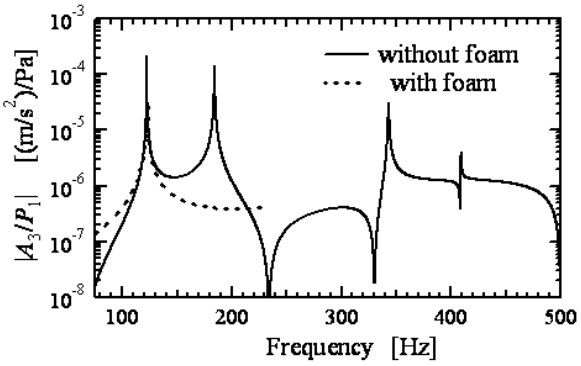

Fig. 6 Calculated acceleration of seat frame using internal air model for foam

5. Conclusion

This paper deals with vibro-acoustic analysis using three-dimensional FEM for automotive seat structures having poroelastic materials and metal frames. There are two media (i.e. internal air and a resin block) in the poroelastic materials for the seat. By carrying out numerical analysis related to the model test, the porous materials for the automotive seat have sound absorption effects for cavity resonance in a room. This effect is mainly due to viscosity of internal air in the porous materials. Further the porous materials also have damping effects for the structural resonance of the metal seat frame under impact excitation at the metal frame. This effect is mainly due to viscoelasticity of the resin block in the porous materials. Furthermore, under an acoustic excitation from a speaker, vibration amplitudes of the metal frame increase by attaching the poroelastic materials to the metal frame. It is " an effect of a sail'' of the resin block in the poroelastic material, which increases vibration level of the seat metal frame by receiving sound pressure. This effect can be simulated using Biot model for the poroelastic materials, which have coupling effects between the elastic deformations of the resin block and the acoustic waves in the internal air.

References

[1] P. Chen and G. Ebbitt, "Noise absorption of automotive seats". ***SAE paper***, 980659, pp.117-121, 1998.

[2] M. A. Biot, "Theory of propagation of elastic waves in a fluid-saturated porous solid (1.Low-frequency range) ", ***Journal of the Acoustical Society of America***, Vol. 28, No. 2, pp.168-178, 1955.

[3] Y. J. Kang and S. Bolton, "A finite element model for sound transmission through foam-lined double panel structures", ***Journal of the Acoustical Society of America***, Vol. 99, pp.2755-2765, 1996.

[4] [4] Y. J. Kang and S. Bolton, "Finite element modeling of isotropic elastic porous materials coupled with acoustical finite elements", ***Journal of the Acoustical Society of America***, Vol.98, No.1, pp.635-643, 1995.

[5] N. Attala, R. Panneton and P. Debergue, "A mixed pressure-displacement formulation for poroelastic materials", ***Journal of the Acoustical Society of America***, Vol.104, No.3, pp.1444-1452, 1998.

[6] J.F. Allard and N. Atalla, ***Propagation of Sound in Porous Media(Second Edition)***, A John Wiley and Sons, Ltd., Publication, 2009.

[7] O. C. Zienkierwicz and Y. K. Cheung, ***The Finite Element Method in Structural and Continuum Mechanics***, McGraw-Hill, 1967.

[8] T. Yamaguchi, Y. Kurosawa and S. Matsumura, "FEA for damping of structures having elastic bodies, viscoelastic bodies, porous media and gas", ***Mechanical Systems and Signal Processing***, Vol.21, No.1, pp.535-552, 2007.

[9] T. Yamaguchi, Y. Nakamoto, Y. Kurosawa and S. Matsumura, "Dynamic analysis of dissipated energy for automotive sound-proof structures including elastic body, viscoelastic body and porous body using FEM in sound bridge phenomena", ***Journal of Environment and Engineering***, Vol.2, No.2, pp. 315-326, 2007.

[10] T. Yamaguchi, Y. Kurosawa and H. Enomoto, "Damped vibration analysis using finite element method with approximated modal damping for automotive double walls with a porous material", ***Journal of Sound and Vibration***, Vol.325, pp.436-450, 2009.

[11] H. Utsuno, T. W. Wu, A. F. Seybert and T. Tanaka, "Prediction of sound fields in cavities with sound absorbing materials", ***AIAA Journal***, Vol.28, No.11, pp.1870-1875. 1990.

[12] Y. Kagawa, T. Yamabuchi and A. Mori, "Finite element simulation of an axisymmetric acoustic transmission system with a sound absorbing wall", ***Journal of Sound and Vibration***, Vol.53, No.3, pp.357-374, 1977.

[13] A. Craggs, "Finite element model for rigid porous absorbing materials", ***Journal of Sound and Vibration***, Vol. 61, No.1, pp.101-111, 1978.

[14] C. Zwikker and C. A. Kosten, ***Sound Absorbing Materials***, Elsevier Press, 1949.